Thermochimica Acta, 74 (1984) 151–166
Elsevier Science Publishers B.V., Amsterdam – Printed in The Netherlands

PARTICLE SIZE EFFECTS IN TEMPERATURE PROGRAMMED TOPOCHEMICAL REACTIONS

K.H. TONGE

School of Chemistry, Robert Gordon's Institute of Technology, St. Andrew Street, Aberdeen, AB1 1HG (Gt. Britain)

(Received 14 September 1983)

ABSTRACT

Contracting solids models for a topochemical process have been combined with the Arrhenius equation and a linear temperature rise equation in a computer program which simulates the reaction rate vs. temperature data such as would be obtained from differential thermogravimetry and temperature programmed reduction techniques. An investigation of the effects of varying the parameters in the model (viz., activation energy, pre-exponential factor, starting temperature, heating rate, particle size and particle size distribution) has shown that the changes brought about by reparameterization may be so subtle that it is unlikely that a single experiment could yield reliable information on any one parameter. The effects of particle size and particle size distribution are shown to be of considerable importance. Attempts have been made to test some of the features revealed in the simulation studies by using nickel oxide powders in hydrogen reduction reactions.

INTRODUCTION

Sustained interest in temperature programmed reaction techniques, particularly as a means of kinetically characterizing reactions of solids is indicated by the large number of papers which continue to appear [1]. Over the last few years temperature programmed reduction (TPR) has come to the fore as a sensitive and convenient technique for the study of reducible species in catalysts, minerals and similar materials. Kinetically, TPR has much in common with thermogravimetry and differential thermal analysis. Comprehensive reviews of the theory, practice and applications of the TPR method have been made by Hurst et al. [2]. The authors explain how mathematical models of real systems undergoing temperature programmed reactions may become so complex that data matching cannot reliably produce parameters of physico-chemical significance. For this reason TPR is best treated as a 'fingerprinting' technique of value in comparative studies. In such studies, variations in the TPR profiles of similar materials measured under the same experimental conditions have been attributed to mixing of oxides [3,4],

0040-6031/84/$03.00

mechanistic changes [5] and support effects [6]. The possibility of particle size variations being responsible for changes in TPR curves has been recognized [7] but in practice may be referred to in only a qualitative way [8,9]. It is well known that the particle size of oxides is greatly influenced by preparative conditions [10] and that this may subsequently have a significant effect in temperature programmed reactions [11]. Changes in dispersion of oxides are also brought about by the presence of impurities [12] and by the effects of supports [13].

In studies of topochemical reactions assumptions are often made, explicitly or implicity, about particle size and size distribution. Hurst et al. [2] urge caution when interpreting isothermal rate measurements which obey the contracting sphere model. In fact obedience to this model, as indicated by a straight line plot of $1 - (1 - \alpha)^{1/3}$ vs. t where α is the fraction reacted, should generally be regarded as purely fortuitous since in most normal systems the 'rate constant' for such a process should be time dependent. This is because the experimental rate constant is inversely proportional to particle size. Normal powdered materials are polydisperse and in such a system, clearly the smallest particles will undergo complete reaction first and the largest particles will survive longest. Thus, unless the extent of reaction is small, the usual contracting sphere plot, which supposes a constant number of spheres, will in this case be curved.

In a temperature programmed situation the effect of change, during the course of reaction, of size distribution on the reaction profiles of materials which are identical in all respects other than their initial dispersity may be very significant.

In this paper, the magnitudes of particle size and size distribution effects in temperature programmed reactions and in the isothermal rate laws used to model these are explored by simulation and experiment.

APPARATUS

Computer programs were written in FORTRAN IV and utilized the GINOF and GINOGRAF libraries for graphical output.

Temperature programmed reduction was performed using an apparatus of overall design similar to that described by Hurst et al. [2] in Fig. 5 of their review. Specific details are as follows: (i) the reducing gas was 5% H_2 in N_2, used at a flow rate of 18 cm^3 min^{-1}. The gas was essentially at atmospheric pressure in the reactor since back pressure in the units downstream of the reactor was very low. (ii) The reducing gas was pretreated by passage through a tube containing about 20 cm^3 of Ni/SiO_2 catalyst at 300°C and a methanol/CO_2 cold trap. (iii) The reactor (Fig. 1) was essentially a U-tube design constructed of transluscent silica. A helical gas preheater tube and a removable thermocouple sheath were incorporated. Approximately 5 mg

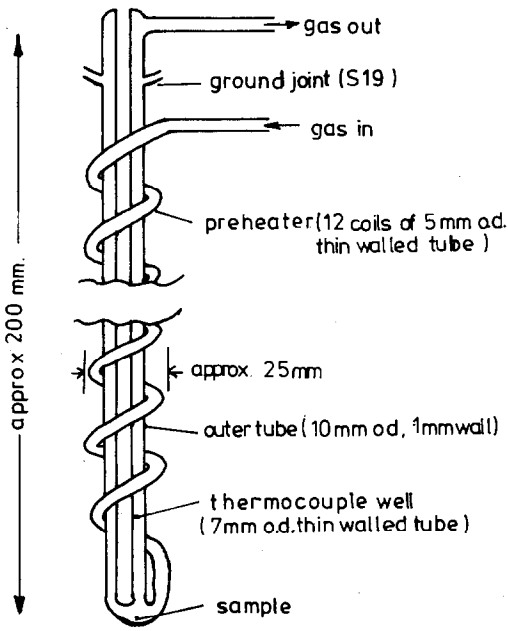

Fig. 1. The all-silica reactor.

samples of oxide were used. Below this size the peak position was virtually independent of sample size. (iv) The vertical reactor furnace was powered by an Ether controller/saturable reactor system. The heating rate was fixed at 6.6 ± 0.5 K min^{-1}. (v) Gaseous reduction products were removed from the gas stream by a liquid nitrogen cold trap. (vi) The hydrogen concentration change was measured by means of a catharometer detector from a Perkin–Elmer 452 gas chromatograph. The sensitivity of the detector and the chart speed were such that 0.1 μmol of H_2 consumed gave a peak about 25 cm^2 in area. Tests on a number of samples showed the peak area to be directly proportional to sample weight.

Isothermal gravimetric studies of NiO reduction were carried out using a thermobalance based on a C.I. Electronics Ltd. microbalance. 5–10 mg samples of oxide were reduced in 100% hydrogen. The oxide sample was held in a platinum crucible inside a furnace, 0.8 cm diameter × 2.5 cm long, totally immersed in the gas stream. The furnace reached the required temperature about 2 minutes at most after switching on the power. The problem of the uncertainty during this initial non-isothermal period was resolved in two alternative ways. Frequently, the fractional weight loss did not amount to more than 0.1 during the heating period and there was little indication of a significant nucleation or acceleratory phase. In this case the weight loss curve was extrapolated back by eye through the non-isothermal region to a notional zero time. In other cases where there was a significant

acceleratory phase the contracting solids equations, which were the subject of the investigations, were applied to the deceleratory region of the weight loss curve by establishing an arbitrary zero weight loss and time point at the start of this region. This rather obvious procedure will be seen to be of significance in the discussion of the results, since the particle size distribution at this arbitrary zero point will clearly be different from that of the original solid.

Particle size analyses were mainly carried out using the Coulter counter Model ZB, but some analyses were carried out using an Andreason pipette and also some by optical microscopy.

MATERIALS

Samples of nickel oxide were prepared by heating one gram quantities of nickel oxysalts (nitrate, oxalate and formate) in air, in shallow crucibles. Heating at different temperatures and for different times produced a variety of oxides for study. The oxides from the oxalate and formate were fine powders but the nitrate produced a granular material which was crushed to < 200 BS 75 μm prior to reduction studies being carried out.

RESULTS AND DISCUSSION

Isothermal reaction studies

The fraction reduced (α) vs. time (t) curves for nickel oxide samples prepared below about 800 K showed good agreement with the contracting sphere equation

$$1-(1-\alpha)^{1/3}=kt \qquad (1)$$

A typical result is shown in Fig. 2 where the straight line (dashed) shows that the experimental data obey eqn. (1) from $\alpha = 0$ (actually $\alpha = 0.25$ since the first 25% of reaction was acceleratory) up to $\alpha = 0.9$. In other cases the fit was often better. In particular, the oxides prepared by the low temperature ignition of nickel nitrate gave straight lines on similar plots from extrapolated notional starting points up to more than 90% reaction. The continuous curves shown in Fig. 2 are the theoretical plots obtained when particle size distribution is taken into account when applying eqn. (1). These comparative curves are discussed fully later.

The rate constants, k, from experiments at different temperatures gave Arrhenius activation energies which varied from about 85 kJ mol^{-1} (1 hour ignition of formate at 673 K) up to 165 kJ mol^{-1} ($\frac{1}{2}$ hour ignition of oxalate at 673 K). The oxides produced from the nitrate gave activation energies of

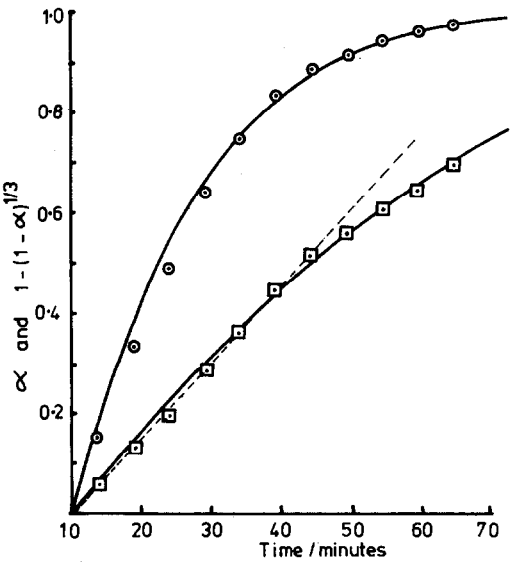

Fig. 2. Product from thermal decomposition of nickel oxalate. Reduction in H_2 at 471 K. Comparison of experimental results with contracting sphere model. ⊙, α vs. t; ⊡, $1-(1-\alpha)^{1/3}$ vs. t; - - - - - -, "good straight line"; ————, curves derived allowing for particle size effect.

about 100 kJ mol^{-1}, similar to values reported by other workers [7,14,15] who also found that the value varied with the preparation temperature of the oxide [15].

Simulations of temperature programmed reactions

The fact that a simple isothermal rate law was often so well obeyed in the nickel oxide reduction suggested that this reaction might be a suitable model process for study by temperature programmed methods.

The incorporation of the Arrhenius equation and a linear heating rate equation into isothermal rate laws gives rise to equations describing temperature programmed reaction profiles. In the case of a contracting cube model with instantaneous nucleation, for example, the reaction rate, which is the rate of decrease of volume, V, of the solid is

$$\frac{dV}{dt} = \frac{d(x_0 - 2kt)^3}{dt} \tag{2}$$

where k is the linear rate of movement of the reaction interface and x_0 the initial side length. Incorporating the Arrhenius equation in the form

$$k = A \exp(-E/R(T_0 + \beta t)) \tag{3}$$

where β is the heating rate and T_0 the initial temperature gives

$$\frac{dV}{dt} = 6x_0^2 A \exp[-E/R(T_0 + \beta t)] - 24x_0 tA^2 \exp[-2E/R(T_0 + \beta t)] + 24t^2 A^3 \exp[-3E/R(T_0 + \beta t)] \tag{4}$$

Note that the adoption of eqn. (2) as the isothermal rate law results in k, and hence A, having units of m s^{-1}.

In a TPR system (as in DTG) the peak height would be proportional to dV/dt.

Interactive computer programs utilizing eqn. (4) (and the analogous contracting sphere equation which shows the same behaviour) allowed investigation of the effects on the dV/dt (i.e. peak height) vs. T curve of varying the parameters x_0, A, E, β and T_0. In the program, a Newton–Raphson iterative method was used to calculate the time taken for a particle of a given size to reach vanishing point so that calculation for that size could be stopped at that point. This feature allowed the program to be adapted as described later to deal with mixtures of different sized particles. Output from the program was available in differential form (as found in DTG and TPR methods) and cumulative form (as found in TG methods) and could be tabular or graphical.

Several series of simulations were carried out in which the parameters were varied over the following ranges

x_0 1–1000 μm
A 10^{-1}–10^5 m s^{-1}
E 50–200 kJ mol^{-1}
β 0.5–25 K min^{-1}
T_0 290–400 K

The following general observations were made with regard to the effects of varying these parameters in monodisperse systems.

The peak width and the temperature of the peak maximum were increased by (i) increasing E, (ii) increasing x_0, (iii) increasing β, (iv) decreasing A. Identical curves can be produced by the model equation with different combinations of these parameters. The curves and the effects observed were very similar to those reported by Wendlandt [16] to have been found in DTA simulations.

The effect of changing T_0 could be relatively insignificant. A difference of 10 K at a T_0 of about 300 K shifted a peak in the 700–800 K region by some 2 K. Thus, provided the reactor of say a TPR apparatus is always equilibrated at room temperature before the start of a run no great error will be introduced by normal ambient temperature fluctuations. Where only a single furnace is available on the equipment this may require considerable patience on the part of the operator. Premature initiation of an experiment with the furnace at say 400 K could cause a shift of 20 K in a peak in the 700–800 K range.

During their development, the programs were checked for correct operation not only by hand calculation but also by subjecting the graphically output results to three mathematically sound methods of analysis frequently used for the determination of activation energies. Two of the methods utilize the effect of varying heating rate [6,17] and the third uses the known

isothermal rate law in a peak width based calculation [18]. Each method gave good agreement with the activation energy used in parameterizing the model when the simulated TPR curves were analyzed using realistic techniques for reading peak temperatures and widths. For example, a set of twenty curves was produced using an activation energy of 100 kJ mol^{-1}, and a pre-exponential factor of 0.1 m s^{-1}. The heating rate was varied from 1 to 20 K min^{-1} and particle size from 1 to 100 μm. When applied to the set of curves, Friedman's method gave $E = 99.5 \pm 2$; Gentry, Hurst and Jones' $E = 98.5 \pm 2$ and Szekely, Till and Vârhegyi's $E = 99.5 \pm 2$ kJ mol^{-1}. The $\pm 2\%$ errors found are as expected for a ± 1 K random error in temperature readings. The error found here is smaller than found by Sestak [19] in his analysis of computed curves using the Freeman–Carroll, Horowitz–Metzger and Doyle methods. Obviously, considerably larger errors could be expected when analyzing real data for the purposes of activation energy determination.

Simulations incorporating particle size distributions

The computer program incorporating eqn. (4) was extended to deal with systems containing a number of independent reacting particles of different sizes. The TPR profile for each size was calculated and the results summed using the input number frequency data. From the studies of the effect of particle size in monodisperse systems it was realized that multiply-moded distributions would give rise to reaction profiles with multiple peaks. Curves for systems consisting of two sizes of particle with a size ratio of 1 : 10 are

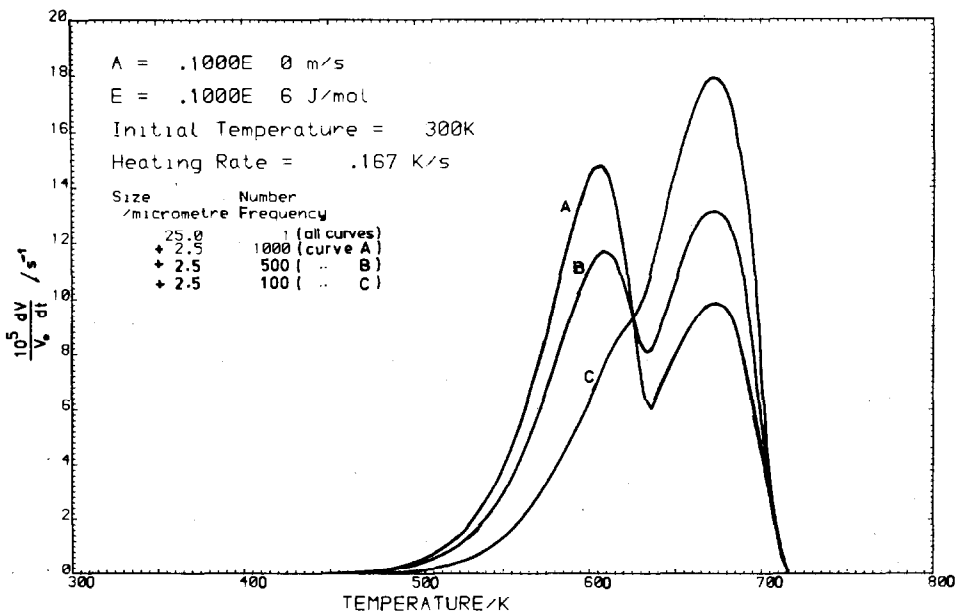

Fig. 3. Simulated TPR profiles of bimodally distributed powders.

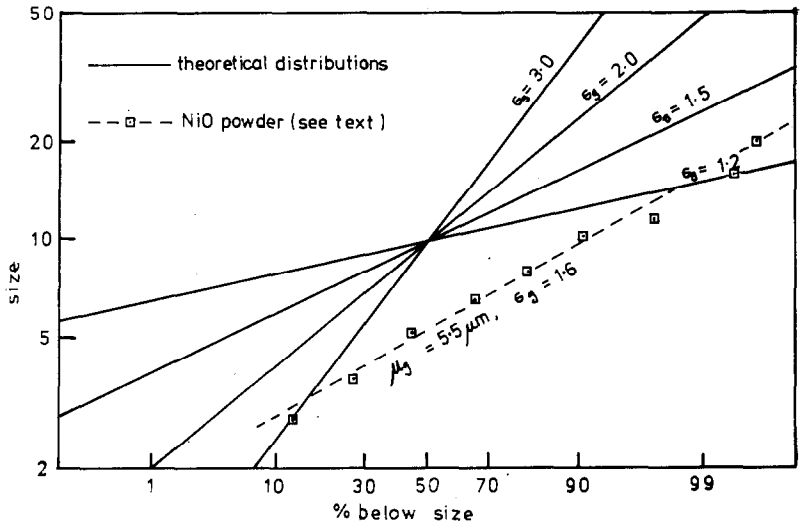

Fig. 4. Log-normal distributions on log-probability scales. ————, theoretical distributions used in simulations; - - ⊡ - -, product from nickel oxalate decomposition.

shown in Fig. 3. Even when the smaller size contributes only 10% to the total volume of solid (curve c) significant distortion of the major peak is observed.

Natural particulate materials are usually much less discretely classified than this. The log-normal law finds frequent use as a smooth function descriptive of size distributions in particulate systems. Using the log-normal law a distribution is completely characterized by two parameters, namely the geometric mean size μ_g, and the geometric standard deviation, σ_g. A log-normal size distribution yields a straight line on log-probability graph paper. A set of lines for powders having $\sigma_g = 1.2–3.0$ and $\mu_g = 10$ is shown along with data for one of the NiO powders in Fig. 4. This material was fairly typical of the products obtained by thermal decomposition of oxalate and formate at lower temperatures. It can be seen that the size distribution is log-normal with $\mu_g = 5.5$ μm and $\sigma_g = 1.6$. In other cases the values ranged from 5 to 20 μm and 1.2 to 1.6 respectively, as measured by Coulter Counter.

For the purposes of a systematic study of size distribution effects the log-normal law itself might have been incorporated into the simulation. However, in this study, the model size distributions shown in Fig. 4 were approximated by constant range width histograms derived from the cumulative distribution data. The histogram data used in simulations are shown in Table 1. This method of approach allowed the simulation program to be used later with real particle size distributions which did not exactly conform to the log-normal law.

In the log-normal histograms, as the value of σ_g increases the distribution becomes more skewed so that the mode moves to smaller values and the size range extends to larger sizes. The effect this has on the temperature pro-

TABLE 1

Constant range width histogram data used in simulations

$\sigma_g = 1.2$		1.5		2.0		2.5		3.0	
Size	Freq.	Size	Freq.	Size	Freq.	Size	Freq.	Size	Freq.
17.5	1	35	1	39	0.5	29	7	27	8
16.5	4	33	2	37	1	27	11	25	11
15.5	8	31	3	35	1.5	25	15	23	20
14.5	20	29	4	33	2	23	20	21	25
13.5	55	27	6	31	3	21	26	19	30
12.5	105	25	7	29	4.5	19	33	17	38
11.5	155	23	10	27	6	17	47	15	43
10.5	195	21	12	25	8	15	58	13	56
9.5	205	19	16	23	10.5	13	66	11	68
8.5	195	17	23	21	13.5	11	80	9	80
7.5	91	15	34	19	17.0	9	90	7	94
6.5	24	13	60	17	21.5	7	111	5	118
5.5	2	11	90	15	27	5	135	3	135
		9	110	13	35	3	120	1	100
		7	92	11	48	1	30		
		5	44	9	62				
		3	4	7	78				
		1	1	5	54				
				3	23.5				
				1	6				

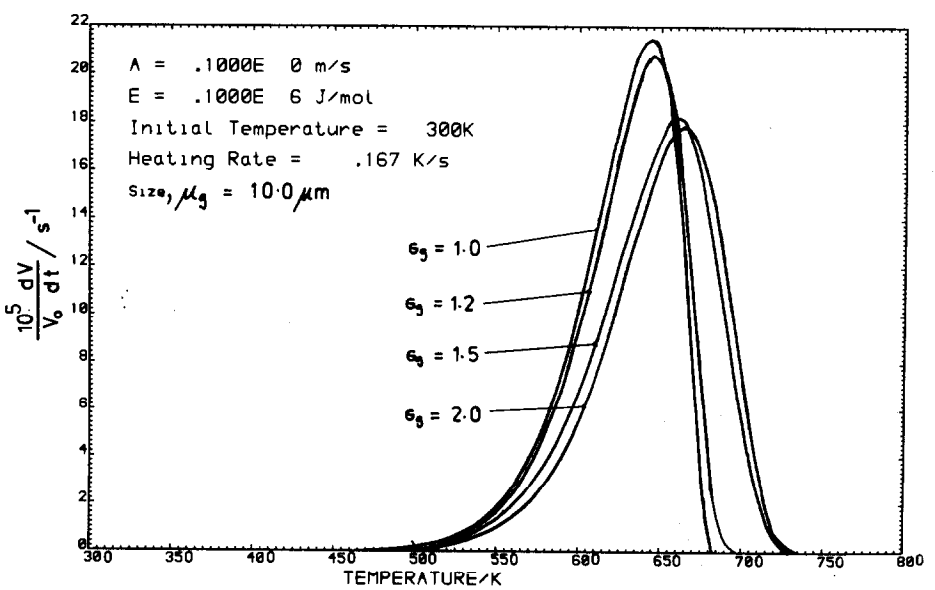

Fig. 5. Effect of varying σ_g on simulated TPR profiles.

grammed reaction profile is shown in Fig. 5. As σ_g increases the peak maximum moves to higher temperatures.

For any given size distribution, the effects of varying E, A, β and T_0 are qualitatively the same as for monodisperse systems.

A series of simulations on a system with $\mu_g = 10$ μm, $\sigma_g = 2.5$ and using different heating rates was carried out. In each case the activation energy was set to 100 kJ mol^{-1}. When the curves were analyzed as had been done for the monodisperse systems using the same three methods it was found that the methods of Gentry et al. [6] and of Friedman [17], which do not depend on the isothermal rate law, gave good agreement with the model activation energy as before. However, the method of Szekely et al. [18] gave values which were about 5–10% lower. The reason for this is clearly that when a size distribution is present the simple contracting solid equations (1) and (2) no longer hold as the isothermal rate law for the powder as a whole.

Effect of size distribution in the isothermal reduction of nickel oxide powders

Reconsidering the results reported in the section on isothermal reaction studies, where it was seen that the reduction of the NiO powders (which are polydisperse) obeys the $\frac{1}{3}$ power law so well, the question arises: What deviations from this law result from the presence of a size distribution? The answer to this question does not yet appear to have been sought through simulation studies although the effect of particle size itself has been noted [20] in reactions where nucleation is not instantaneous.

A computer program to simulate the reactant volume vs. time behaviour of an isothermally reacting polydisperse system of spherical particles was written and run with log-normal size distributions having $\mu_g = 10$ and $\sigma_g = 1.0$–3.0. Some of the results are shown in Fig. 6. The results for $\sigma_g = 2.0$ to $\sigma_g = 3.0$ were not very different from the $\sigma_g = 1.5$ result shown. The curves show that even in the most extreme case, given the usual licence employed by workers in the field of solid state reaction kinetics, a "good straight line" is found for α values up to 0.7. It should be noted that, compared to the perfect straight line of the $\sigma_g = 1.0$ case, when a size distribution is present the contracting sphere function gives a curve which starts off more steeply and then curves down at high α values. This is what is actually found when such plots are made for real powders (Fig. 2).

The oxide which gave the results shown in Fig. 2 was found by Coulter Counter measurements to have $\mu_g = 5.5$ μm and $\sigma_g = 1.6$. The number frequency vs. size data are those shown in Fig. 4. As can be seen the log-normal distribution law appears to be reasonably well obeyed over the range of measurement used. The actual Coulter Counter number frequency vs. size data for this oxide were used in the isothermal contracting sphere simulation program and yielded the results indicated by the smooth curves in Fig. 2 when suitably time-scaled by the appropriate choice of rate

constant. The excellent agreement between the experimental results and the simulation shows that polydispersity of the sample is sufficient to explain the pronounced deceleratory phase. It is not necessary to invoke a change in the reaction mechanism to account for the final stage in the reaction.

It should be noted that in this particular case the contracting sphere equation was applied to only the last 75% of the reaction since the first 25% was acceleratory. It can be shown easily that although the size distribution of a powder is changed by a 25% weight loss it is still virtually log-normal. μ_g becomes slightly smaller and σ_g slightly larger. In the case being considered here the change was from $\mu_g = 5.5$ μm, $\sigma_g = 1.6$ to $\mu_g = 4.5$ μm, $\sigma_g = 1.7$. Although the data characterized by these former parameters were shown in Fig. 2 the differences between these and the curves corrected for size loss are insignificant, indeed any curves for σ_g between about 1.5 and 2.0 could be made to give a reasonable fit to the experimental results by suitable time scaling. This lack of sensitivity to changes in σ_g does not invalidate the general conclusion that size distribution alone can account for the kinetics.

Temperature programmed reduction of NiO powders

A number of NiO powders, variously prepared, were investigated by the TPR method. Virtually all the preparations gave peaks in which the temperature of maximum rate, T_m, lay between 590 and 670 K. Although the TPR profiles of given samples were quite reproducible, the preparations themselves were less so. However, the general tendency is for T_m to increase with increased preparation temperature up to a preparation temperature of about 500°C. Beyond this T_m occurs at slightly lower values. Samples prepared at

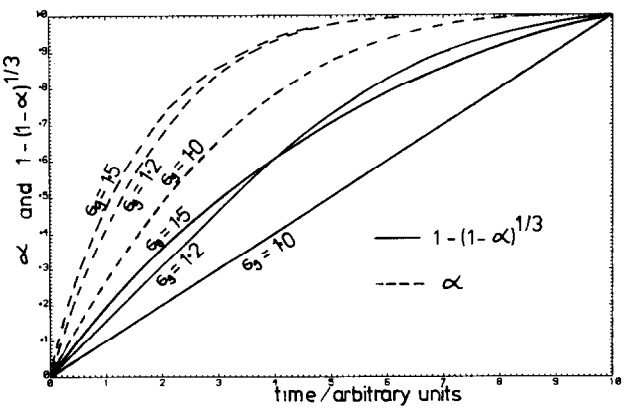

Fig. 6. Effect of particle size distribution on the applicability of the contracting sphere equation.

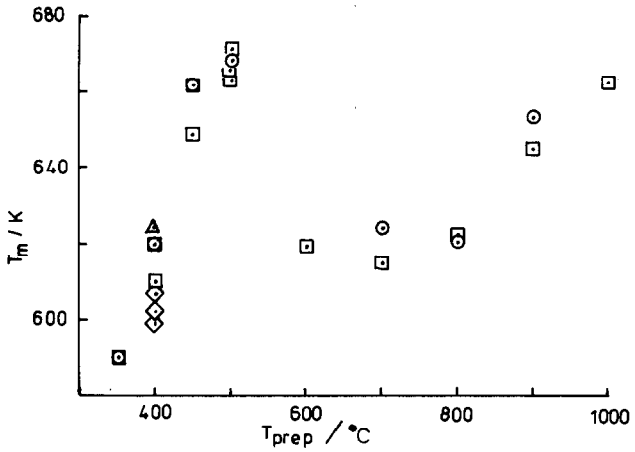

Fig. 7. Peak temperatures, T_m, in the TPR of various NiO samples. Products from ◇, oxalate; ⊙, ⊡, nitrate (two different operators); ⧋, formate.

about 800°C or higher show increasing T_m values and in some cases the peak is broader and flatter for these samples. The T_m values of the various preparations are shown in Fig. 7. The variation in T_m with preparation temperature does not correlate with the specific surface area variations as determined by nitrogen adsorption (Table 2). The samples prepared at 500°C or less certainly show increasing T_m as the surface area decreases (i.e. as particle size increases), as do the T_m values for the 600°C and higher temperature preparations. The discontinuity between 500 and 600°C is not, however, reflected in the surface area data.

To demonstrate positively the dependence of T_m on particle size, NiO powder produced from the oxalate at 400°C was fractionated by sedimentation in water. The TPR profiles of the products from which larger particles had been eliminated are shown in Fig. 8.

TABLE 2

Specific surface areas of NiO powders

T_{prep}(°C)	Surface area (m^2g^{-1})
400 *	40
400	55
450	15
500	13
600	3
700	6
800	7
900	~2
1000	~1

* Prepared from Ni oxalate, all others prepared from Ni nitrate

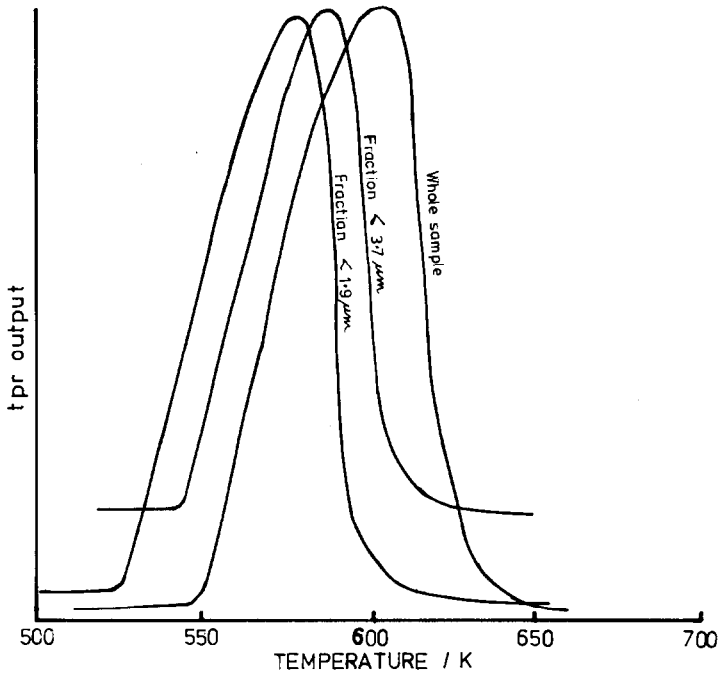

Fig. 8. Effect of particle size on the TPR profile of NiO.

It is clear from these results that, in agreement with simulation studies, both T_m and the initial peak temperature increase as average particle size increases.

Practically demonstrating the effects of varying geometric standard deviation has proved elusive. All the oxide powders produced, whether analysed by optical microscopy, Coulter Counter or Andreason pipette gave approximately log-normal distributions. Using the experimental size vs. frequency data in simulations of TPR for these oxides gave the same smooth types of curve as found for the exact log-normal systems such as those in Fig. 5. The experimental TPR curves were, however, often far from smooth. Many showed the same kind of irregularities found by other workers in the case of nickel oxide and other oxides in pure, doped and supported forms [2,3]. Fig. 9 shows two representative TPR profiles of a less regular nature. A typical TPR profile of a more regular nature is shown in Fig. 10. The oxide here is that referred to in Figs. 2, 4 and 9. Superimposed is the simulated curve obtained using the experimental size distribution and the activation energy found from isothermal studies. By using the pre-exponential factor as a variable parameter it has been possible to match the peak temperature, but for the most part the model fails to reproduce the experimental result. There are several possible reasons for this. These are

(a) Experimental errors associated with the TG and TPR equipment.

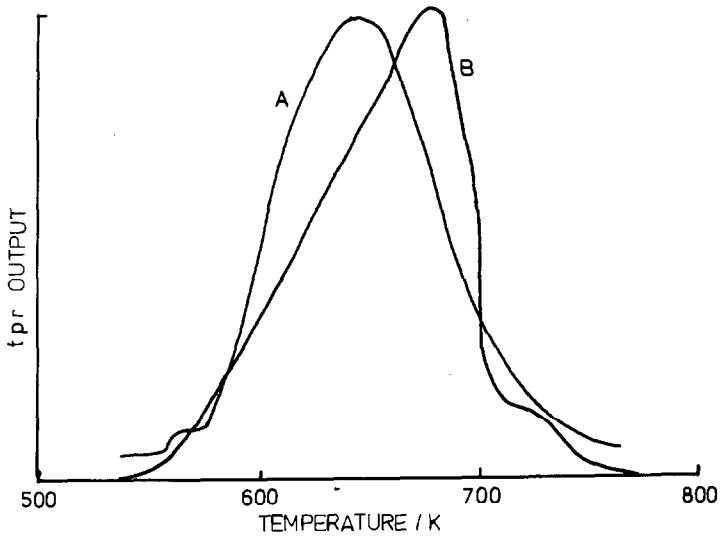

Fig. 9. TPR profiles showing bumpy irregularities. A, product from Ni formate; B, product from Ni nitrate.

(b) Insensitivity of the particle size distribution analysis methods.
(c) Invalidity of the contracting solid isothermal rate law.

Apart from the uncertainties in the first non-isothermal or acceleratory period of isothermal reaction there remains a question as to whether the

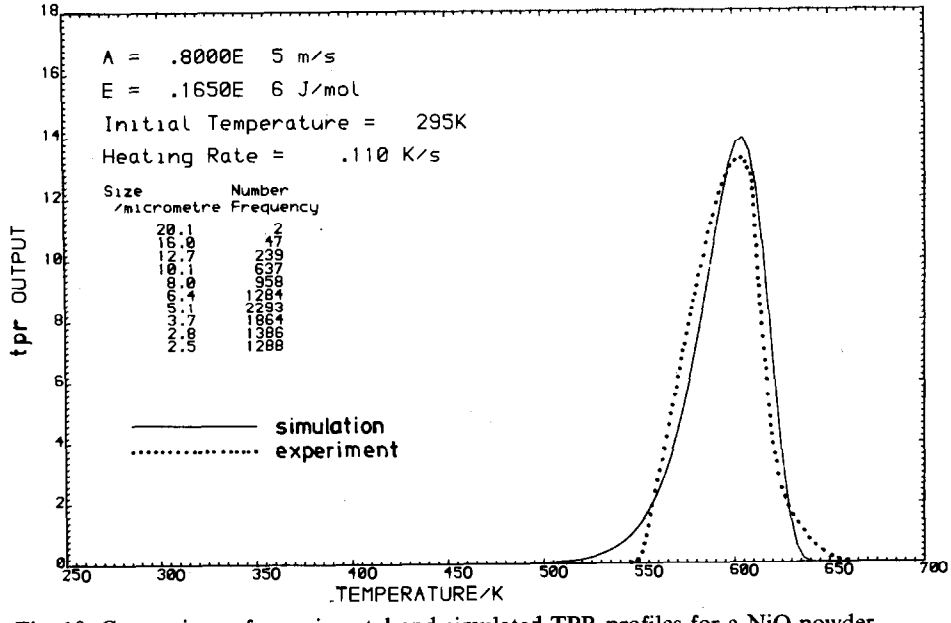

Fig. 10. Comparison of experimental and simulated TPR profiles for a NiO powder.

good fit of the cube root law is merely fortuitous. Electron photomicrographs of the powders show them to consist of very irregularly shaped particles. Also it should be noted that the surface areas of the powders as determined by nitrogen adsorption are many times larger than suggested by the particle size analysis results. A recurrent feature of the adsorption/desorption isotherms of the powders was the presence of a hysteresis loop indicating that particles may be porous. Even were the contracting sphere law a true reflection of the topochemical nature of the reduction reaction, its use in conjunction with a constant pre-exponential factor in non-isothermal studies may be invalid when the heating rate is linear [21].

(d) Invalidity of the Arrhenius equation

Isothermal experiments used to find the rate law and activation energy were conducted over only a small range of temperature. There is no evidence to suggest that either is valid over the larger range of temperatures covered in a TPR experiment. That there may be little justification for making such assumptions, particularly in the case of solid state reactions has been demonstrated and discussed many times [22–24].

CONCLUSIONS

In these studies it has been shown both practically and by simulation that particle size distribution can account for the isothermal kinetics of a topochemical process. Practical demonstration of the particle size distribution effects predicted by simulations of temperature programmed reactions has proved difficult. Nevertheless, despite the uncertainties, it is reasonable to suppose that size distribution effects could account for the different TPR behaviour of oxides which have been prepared in nearly identical ways. The same ideas would apply to other non-isothermal methods of studying topochemical processes.

ACKNOWLEDGEMENTS

Thanks are due to my colleagues Dr. R. McCosh, who initiated the TPR work, Mr. J. Harper for useful discussions and also to many students, especially Mr. W. Wilson and Miss C. Wilson, who did much of the groundwork.

REFERENCES

1 See for example D. Dollimore (Ed.), Proceedings of the Second European Symposium on Thermal Analysis, Heyden, London, 1982. Eleven papers deal directly with non-isothermal kinetics.

2 N.W. Hurst, S.J. Gentry, A. Jones and B.D. McNicol, Catal. Rev. Sci. Eng., 24 (1982) 233.
3 S.D. Robertson, B.D. McNicol, J.H. de Baas, S.C. Kloet and J.W. Jenkins, J. Catal., 37 (1975) 424.
4 N. Wagstaff and R. Prins, J. Catal., 59 (1979) 434.
5 S.J. Gentry, N.W. Hurst and A. Jones, J. Chem. Soc., Faraday Trans. 1, 77 (1981) 603.
6 S.J. Gentry, N.W. Hurst and A. Jones, J. Chem. Soc., Faraday Trans. 1, 75 (1979) 1688.
7 M. Bulens, Ann. Chim. (Paris), t. 1, No. I (1976) 13.
8 T. Paryjczak, J. Goralski and K.W. Jozwiak, React. Kinet. Catal. Lett., 16 (1981) 147.
9 J.W. Jenkins, Canadian Symposium on Catalysis, 6 (1979) 21.
10 C.J. Keattch and D. Dollimore, An Introduction to Thermogravimetry, 2nd edn., Heyden, London, 1975, p.113.
11 C.J. Keattch and D. Dollimore, An Introduction to Thermogravimetry, 2nd edn., Heyden, London, 1975, p. 28.
12 M.E. Dry and F.S. Stone, Faraday Discuss. Chem. Soc., 23 (1959) 192.
13 M. Houalla, F. Delannay and B. Delmon, J. Chem. Soc., Faraday Trans. 1, 76 (1980) 1766.
14 A. Yamaguchi and J. Moriyama, Mem. Fac. Eng. Kyoto Univ., 28 (1966) 389.
15 P. Clough and D. Dollimore, Vac. Microbalance Technol., 7 (1970) 51.
16 W.W. Wendlandt, Thermal Methods of Analysis, 2nd edn., New York, Wiley, 1974, p. 480.
17 H.L. Friedman, J. Polym. Sci., Part C, 6 (1965) 18.
18 T. Szekely, F. Till and G. Várhegyi, Proceedings of the Second European Symposium on Thermal Analysis, Heyden, London, 1981, p. 135.
19 J. Sestak, Talanta, 13 (1966) 567.
20 C.A. Mampel, Z. Phys. Chem., Abt. A, 187 (1940) 235.
21 G. Gyulai and E.J. Greehow, Talanta, 21 (1974) 131.
22 D. Dollimore, G.R. Heal and B.W. Krupay, Thermochim. Acta, 24 (1978) 293.
23 I.K. Avramov, Thermochim. Acta, 15 (1976) 281.
24 F.C. Tompkins, In G.-M. Schwab (Ed.), Reactivity of Solids, Elsevier, Amsterdam 1964, p. 3.